Institute for Advanced Technology
The University of Texas at Austin

Cavity Expansion Analysis of Brittle Materials

S. Satapathy and S. Bless
Institute for Advanced Technology
The University of Texas at Austin

July 1995

IAT.R 0075

Certification of Technical Review

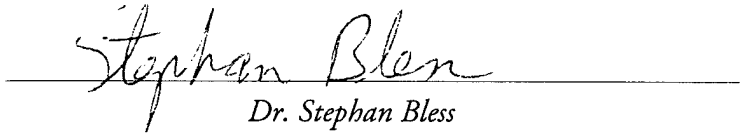

Dr. Stephan Bless

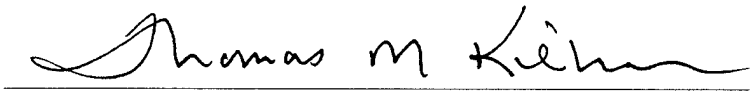

Dr. Thomas Kiehne

REPORT DOCUMENTATION PAGE

Form Approved
OMB NO. 0704-0188

1. AGENCY USE ONLY (Leave blank)	2. REPORT DATE	3. REPORT TYPE AND DATES COVERED
	July 1995	Technical Report

4. TITLE AND SUBTITLE

Cavity Expansion Analysis of Brittle Materials

5. FUNDING NUMBERS

Contract # DAAA21-93-C-0101

6. AUTHOR(S)

S. Satapathy and S. Bless

7. PERFORMING ORGANIZATION NAME(S) AND ADDRESS(ES)

Institute for Advanced Technology
The University of Texas at Austin
4030-2 W. Braker Lane, #200
Austin, TX 78759

8. PERFORMING ORGANIZATION REPORT NUMBER

IAT.R 0075

9. SPONSORING / MONITORING AGENCY NAME(S) AND ADDRESS(ES)

U.S. Army Research Laboratory
ATTN: AMSRL-WT-T
Aberdeen Proving Ground, MD 21005-5066

10. SPONSORING / MONITORING AGENCY REPORT NUMBER

11. SUPPLEMENTARY NOTES

The view, opinions and/or findings contained in this report are those of the author(s) and should not be considered as an official Department of the Army position, policy, or decision, unless so designated by other documentation.

12a. DISTRIBUTION / AVAILABILITY STATEMENT

Approved for public release; distribution unlimited.

12b. DISTRIBUTION CODE

A

13. ABSTRACT *(Maximum 200 words)*

In this report, we show that the 'target resistance' of brittle materials can be calculated accurately using spherical cavity expansion analysis and a conventional brittle material model. The stress field ahead of the tip of the penetrator is assumed to have spherical symmetry. The brittle material is modeled as an elastic material which cracks under tension. The cracked material is considered to be pulverized when it fails in compression, which is then characterized as a Mohr-Coulomb material with pressure dependent shear strength. The target resistance value found from this analysis compares well with the reported experimental values for AD995 alumina (Al_2O_3)

14. SUBJECT TERMS

target resistance, cavity expansion analysis, brittle materials, ceramics, alumina.

15. NUMBER OF PAGES

15

16. PRICE CODE

17. SECURITY CLASSIFICATION OF REPORT	18. SECURITY CLASSIFICATION OF THIS PAGE	19. SECURITY CLASSIFICATION OF ABSTRACT	20. LIMITATION OF ABSTRACT
Unclassified	Unclassified	Unclassified	UL

CAVITY EXPANSION ANALYSIS OF BRITTLE MATERIALS

by

Sikhanda Satapathy and Stephan Bless

1.0 Introduction

Cavity Expansion Models (CEM) have been used to calculate the target resistance (R_t) of materials to penetration. R_t is considered to be the static pressure required to open up a cavity in the target [1, 2]. This approach has been applied successfully for metal targets first by Bishop, Hill, and Mott [3] and more recently by Forrestal, et al. [4]. The merit of this form of closed form analytical solution is that implications of material models can be directly determined without having to first insert them into wavecodes and numerically simulate penetration events. This kind of macroscopic analysis is also helpful in performing parametric studies which can identify important material parameters that affect penetration resistance.

There are very few cavity expansion treatments of brittle materials. Forrestal, et al. [5] used an elastic-cracked-plastic material model to calculate R_t for AD85 alumina. Wright, et al. [6] used an elastic-plastic-hackle material model to calculate R_t for polycarbonate. Partom used an elastic-plastic material model with a pressure dependent strength in the plastic region, which saturates at high pressure, to calculate R_t for AD995 [7]. In this paper we demonstrate that an elastic-cracked-pulverized material model yields R_t values close to experimentally measured values for AD995 alumina [8]. We do not assume any plastic flow in the target material. It is found that the target resistance depends on compressive and tensile strengths and the pressure-shear coefficient of the pulverized material.

2.0 Response Regions

In steady state penetration (after the initial shock phase is over), the penetrator erodes and decelerates due to the stress at the target-penetrator interface. The stress in the target that resists penetration consists of two parts: 1) the inertial stress required to accelerate target material out of the path of the penetrator; and 2) the stress required to deform the target around the cavity. This second term is identified with the target resistance R_t. Partom and Littlefield [9] pointed out that there is also a dependence of R_t on velocity in materials for which the strength depends on pressure, since the pressure is higher in high velocity penetration. That coupling is ignored in this treatment.

The stress field ahead of the penetrator-target interface can be approximated to have spherical symmetry. We model the alumina ceramic as an elastic material which cracks under tension and then pulverizes when the compressive stress exceeds the one dimensional compressive failure strength. The implication of this assumption is depicted schematically in Figure 1 which shows three zones: the region near the cavity is comminuted; next to the comminuted zone there is a "radially cracked" zone (radial cracks are formed because the

hoop stress exceeds the tensile strength); and beyond the "radially cracked" zone the ater i is elastic. This phenomenology is consistent with Collombet and Tranchet's [10] ob vati of explosive cavities in alumina (see Figure 2); they find "intergranular cracks" ar t cavity, next to which "transgranular cracks" were found. The "transgranular cr s" radially oriented which implies that for spherical symmetry, the hoop stress is ze In "intergranular crack" region, the cracks are randomly oriented and are inter nect Essentially, the material in this region is fragmented and comminuted. This s uence of failed regions around the cavity is generally consistent with measurements aluminas penetrated by long rods [11]. Although there are some observations th e level of communition varies in the pulverized zone [12], we model the entire pulveri aterial as a Mohr-Coulomb material with a pressure dependent shear strength. Th ssure-shear coefficient is derived from the uniaxial stress-shear coefficient experimentally obtained by Clifton, et al. [13].

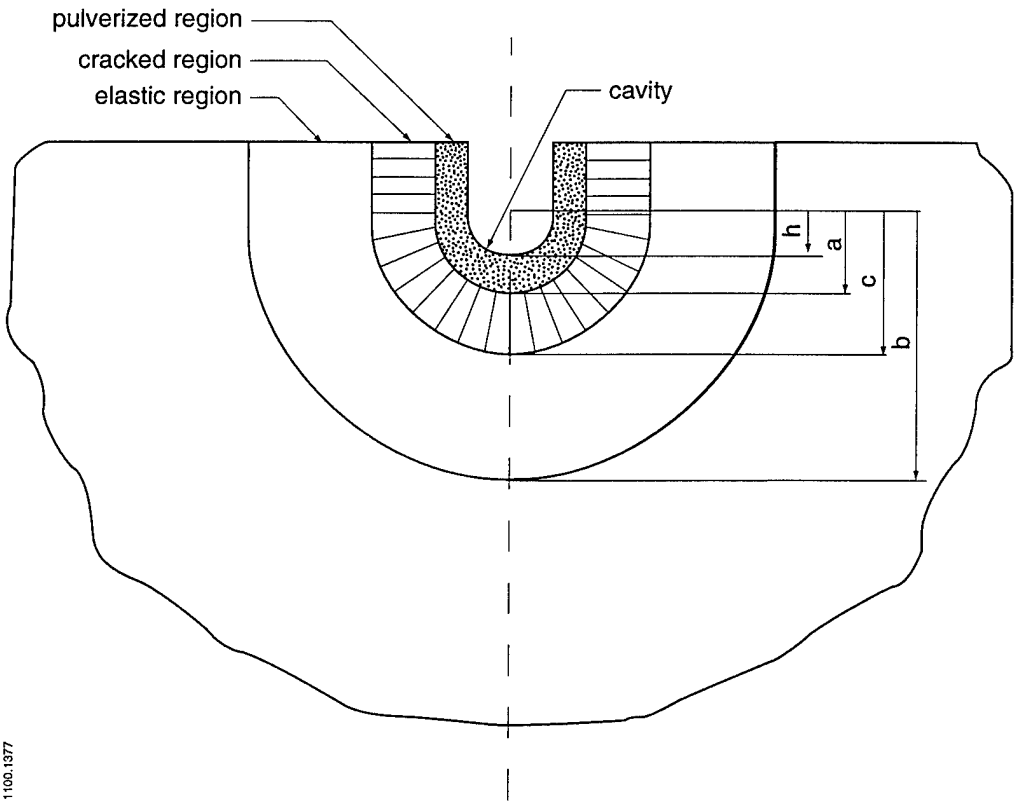

Figure 1. Response regions in the target.

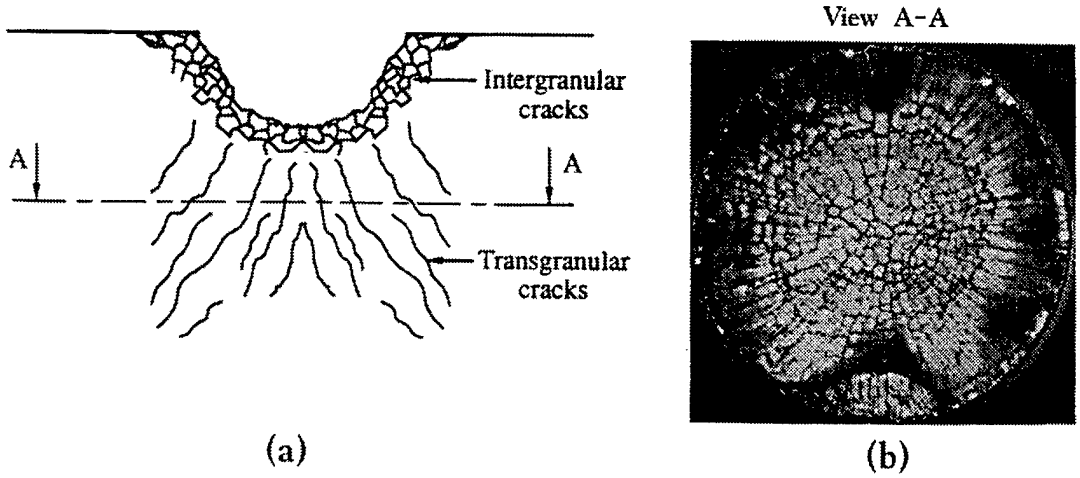

Figure 2(a). Isotropic and anisotropic networks of cracks [10]. 2(b) Transgranular cracks in the soft recovered sample [10].

3.0 Elastic Region

The elastic zone extends from r = c to r = b where b is the stress-free outer boundary of the target. At the cracked-elastic boundary the hoop stress equals the tensile strength of the material. We neglect inertial terms, since R_t, by definition, is the stress required to open a cavity quasi-statically. The field equations can be written as,

Equilibrium equation:
$$\frac{d\sigma_r}{dr} + 2\frac{\sigma_r - \sigma_\theta}{r} = 0 \tag{1}$$

Strain-displacement relation:
$$\varepsilon_r = \frac{du}{dr} \text{ and } \varepsilon_\theta = \varepsilon_\phi = \frac{u}{r} \tag{2}$$

Constitutive relation for elastic region:
$$\varepsilon_r = \frac{1}{E}\left[\sigma_r - 2\nu\sigma_\theta\right] \tag{3}$$

$$\varepsilon_\theta = \varepsilon_\phi = \frac{1}{E}\left[(1-\nu)\sigma_\theta - \nu\sigma_r\right] \tag{4}$$

Equations (2), (3), and (4) can be combined with (1) to yield,

$$\frac{d^2u}{dr^2} + \frac{2}{r}\frac{du}{dr} - \frac{2u}{r^2} = 0 \tag{5}$$

which has a solution of the form:

$$u = c_1 r + \frac{c_2}{r^2} \tag{6}$$

To evaluate c_1 and c_2 we need two boundary conditions which are:

$$\sigma_r|_{r=b} = 0 \tag{7}$$

and

$$\sigma_\theta|_{r=c} = \sigma_f \tag{8}$$

By using (2), (3), and (4), stresses can be expressed as:

$$\sigma_r = \frac{E}{(1+\nu)(1-2\nu)}\left[(1-\nu)\frac{du}{dr} + 2\nu\frac{u}{r}\right] \tag{9}$$

$$\sigma_\theta = \frac{E}{(1+\nu)(1-2\nu)}\left[\nu\frac{du}{dr} + \frac{u}{r}\right] \tag{10}$$

Thus, using (6) to (10), the constants are found to be:

$$c_1 = -\frac{\sigma_f(1-2\nu)}{E\left(1+\frac{b^3}{2c^3}\right)} \tag{11}$$

$$c_2 = -\frac{\sigma_f(1+\nu)b^3}{2E\left(1+\frac{b^3}{2c^3}\right)} \tag{12}$$

Inserting these constants in (6), (9), and (10) yields the following form for the displacement and stresses:

$$u = \frac{\sigma_f}{2E\left(1+\frac{b^3}{2c^3}\right)}\left[(1-2\nu)r + \frac{(1+\nu)b^3}{r^2}\right] \tag{13}$$

$$\sigma_r = \frac{\sigma_f}{\left(1+\frac{b^3}{2c^3}\right)}\left[1-\frac{b^3}{r^3}\right] \tag{14}$$

$$\sigma_\theta = \frac{\sigma_f}{\left(1+\frac{b^3}{2c^3}\right)}\left[1+\frac{b^3}{2r^3}\right] \tag{15}$$

Expressions for the pressure and the shear stress in this elastic region are given by:

$$P = \frac{\sigma_f}{\left(1+\frac{b^3}{2c^3}\right)} \tag{16}$$

$$\frac{1}{2}|\sigma_r - \sigma_\theta| = \frac{3}{4}\frac{\sigma_f}{\left(1+\frac{b^3}{2c^3}\right)}\frac{b^3}{r^3} \tag{17}$$

4.0 Cracked Region

As discussed before, the material will crack when the tensile hoop stress exceeds the tensile strength. Thus the elastic region will be bounded inwardly by a radially cracked region (a < r < c) within which the radial cracks are assumed to be spatially distributed in various sizes in such a manner that the hoop stress in the whole region is zero. The inner boundary of this region is defined by the boundary condition that the material is pulverized. Since the stress state in the cracked region is uniaxial, pulverization occurs where the radial stress exceeds the uniaxial compressive strength, Y; i.e.,

$$\sigma_r|_{r=a} = -Y \tag{18}$$

To be able to use continuum equations in the cracked region (which is in fact discontinuous), we resort to the averaging theorems of micro-mechanics (see Appendix I) which let us apply the continuum equations adopting averaged field variables. Hence the stress and displacements are volume averaged quantities allowing for local variations. Since $\sigma_\theta = 0$, the equilibrium equation (1) reduces to,

$$\frac{d\sigma_r}{dr} + 2\frac{\sigma_r}{r} = 0 \tag{19}$$

which can be integrated with (18) to yield,

$$\sigma_r = -Y\frac{a^2}{r^2} \tag{20}$$

Also since the radial stress has to be continuous at the elastic-cracked boundary, r = c, then from (14) and (20),

$$\left(\frac{c}{a}\right)^2 = -\frac{Y}{\sigma_f}\frac{\left(1+\frac{b^3}{2c^3}\right)}{\left(1-\frac{b^3}{c^3}\right)} \tag{21}$$

To evaluate displacement in the cracked region, Forrestal, et al. [5] have used the equation of state with bulk modulus of the intact material. But in fact, presence of radial cracks will

render the material anisotropic. Thus we can not use the isotropic elastic constants of the intact material to characterize the displacement of this anisotropic cracked region. However, absence of transverse cracks ensures no degradation of elastic moduli in the radial direction.

Hence using (20) with the stress-strain relation in the radial direction, $\sigma_r = E\varepsilon_r = E\frac{du}{dr}$, find,

$$u = \frac{Y}{E}\frac{a^2}{r} + A \tag{22}$$

The constant A is evaluated by using continuity of displacement at r = c. Thus from (13) and (22), we obtain:

$$u = \frac{\sigma_f}{2E\left(1+\frac{b^3}{2c^3}\right)}\left[\frac{(1-2\nu)c^3+(1+\nu)b^3}{c^2}\right] + \frac{Y}{E}\frac{a^2}{c}\left(\frac{c}{r}-1\right) \tag{23}$$

The pressure and shear stress in this region can be written as,

$$P = \frac{Ya^2}{3r^2} \tag{24}$$

$$\tau = \frac{1}{2}|\sigma_r - \sigma_\theta| = \frac{Ya^2}{2r^2} \tag{25}$$

5.0 Comminuted Region

Subject to the same kind of assumptions regarding applying continuum equations to an inherently discontinuous region, we set the shear stress in the comminuted region (h < r < a) equal to the "flow stress," which is taken as pressure dependent. Thus,

$$\frac{\sigma_r - \sigma_\theta}{2} = m\left(\frac{\sigma_r + 2\sigma_\theta}{3}\right) \tag{26}$$

The equilibrium equation (1) reduces to,

$$\frac{d\sigma_r}{dr} + 2\alpha\frac{\sigma_r}{r} = 0 \tag{27}$$

where

$$\alpha = \frac{6m}{3+4m} \tag{28}$$

With the boundary condition (18), (27) can be solved to yield,

$$\sigma_r = -Y\left(\frac{a}{r}\right)^{2\alpha} \tag{29}$$

The target resistance, R_t, which is the negative of the radial stress at the cavity boundary, r = h, is thus found as,

$$R_t = Y\left(\frac{a}{h}\right)^{2\alpha} \tag{30}$$

Finally, the pressure and the shear stress in the comminuted region can be calculated as,

$$P = Y\left(\frac{a}{r}\right)^{2\alpha}\frac{3-2\alpha}{3} \tag{31}$$

$$\tau = \frac{1}{2}|\sigma_r - \sigma_\theta| = \frac{1}{2}\alpha Y\left(\frac{a}{r}\right)^{2\alpha} \tag{32}$$

6.0 Calculation of h/a

From (30), we note that to solve for R_t, we need to evaluate the size of the pulverized zone relative to the cavity size. Even though this ratio turns out to be a constant, independent of geometry for an infinite target, we first derive its value for a finite target. Thus far we have avoided using any constitutive relation for the comminuted region. In the previous section, we integrated the equation of motion with the assumption that the shear stress varies linearly with pressure in this region (Mohr-Coulomb criteria). Even if we assume statistical homogeneity, the elastic moduli may be different from those of the intact material. Holmquist [14] notes that one can ignore the difference between the elastic moduli of intact and pulverized material. Presence of bulking due to comminution complicates the problem further, due to the competition between dilatancy and pore compaction. Curran, et al. [12] observed that dilatancy occurs only after the large compressive stress has disappeared. Thus if we neglect both dilatancy and compaction due to pressure (assuming that they cancel out at least to a first order approximation), we have no volume change in the comminuted region. From the conservation of mass, and ignoring higher order terms in *u(a)*,

$$\frac{1}{3}\left(\frac{h}{a}\right)^3 = \frac{u(a)}{a} \tag{33}$$

Since the radial displacement has to be continuous at r = a, u(a) is given by (23). Thus,

$$\frac{1}{3}\left(\frac{h}{a}\right)^3 = \frac{\sigma_f}{2E\left(1+\frac{b^3}{2c^3}\right)}\left[\frac{(1-2\nu)c^3+(1+\nu)b^3}{c^2 a}\right] + \frac{Y}{E}\left(1-\frac{c}{a}\right) \tag{34}$$

Equation (34) and (21) have two unknowns c and a. For a given geometry (h and b kn n), these two equations can be solved for "a" and the cavity expansion pressure, R_t, c be calculated.

7.0 Infinite Target

For an infinite target (i.e., b is very large), the RHS of (34) is a function of only c which can be evaluated from (21). Thus, the ratio h/a and hence R_t is determined purely om the material constants. By letting $b \to \infty$, (21), (34) and (30) reduce to:

$$\frac{c}{a} = \sqrt{\frac{Y}{2\sigma_f}} \tag{35}$$

$$\frac{1}{3}\left(\frac{h}{a}\right)^3 = \frac{Y}{E}\left[1 - \sqrt{\frac{\sigma_f}{Y}}\frac{(1-\nu)}{\sqrt{2}}\right] \tag{36}$$

$$R_t = Y\left[\frac{\left(\frac{E}{3Y}\right)}{1 - \sqrt{\frac{\sigma_f}{Y}}\frac{(1-\nu)}{\sqrt{2}}}\right]^{\frac{2\alpha}{3}} \tag{37}$$

8.0 Material Constants for Coors AD995 Alumina

We calculate the elastic constants for AD995 alumina from the longitudinal and transverse wave speeds reported by Grady [15] as E = 373.14 GPa, K = 231.8 GPa. The quasi-static strength parameters as published by Coors are: compressive strength, Y = 2.62 GPa; and tensile strength σ_f = 0.262 GPa. Tracy [16] points out that conventional compression tests tend to give strength measurements that are misleadingly low. Using a dumbbell-shaped specimen he measured a compressive strength of 3.5 GPa for AD94 alumina. As a conservative estimate, compressive strength for AD995 should be at least 3.5 GPa. Bar impact tests of similar alumina gives intermediate results [17, 18]. We report R_t for compressive strength of both 2.6 GPa and 3.5 GPa. Finally, to calculate the pressure-shear coefficient, m, we make use of Clifton's [13] experimental value of normal stress vs. shear stress coefficient as follows.

Let $$\frac{1}{2}(\sigma_r - \sigma_\theta) = \mu\sigma_r \tag{38}$$

solving for σ_θ, we obtain,

$$\sigma_\theta = \sigma_r(1 - 2\mu) \tag{39}$$

and hence m is given by:

$$m = \frac{(\sigma_r - \sigma_\theta)/2}{(\sigma_r + 2\sigma_\theta)/3} = \frac{3\mu}{3 - 4\mu} \tag{40}$$

From Clifton's [13] measured value of $\mu = 0.2$, we obtain m = 0.273.

9.0 Results

We plot the R_t value for an infinite target of AD995 alumina as a function of the pressure shear coefficient, m, in Figure 3. For m = 0.273 (from Clifton's data), we find that R_t = 7.7 GPa for Y = 2.62 GPa, and R_t = 9.46 GPa for Y = 3.5 GPa. Subramanian and Bless [8] conducted penetration experiments on AD995 targets with tungsten penetrators and found that Tate's [19] solution using R_t= 8.5 GPa passes through almost all the error bars for the experimental values. Thus, our closed form solution has resulted in R_t values that tightly bracket the experimental observation.

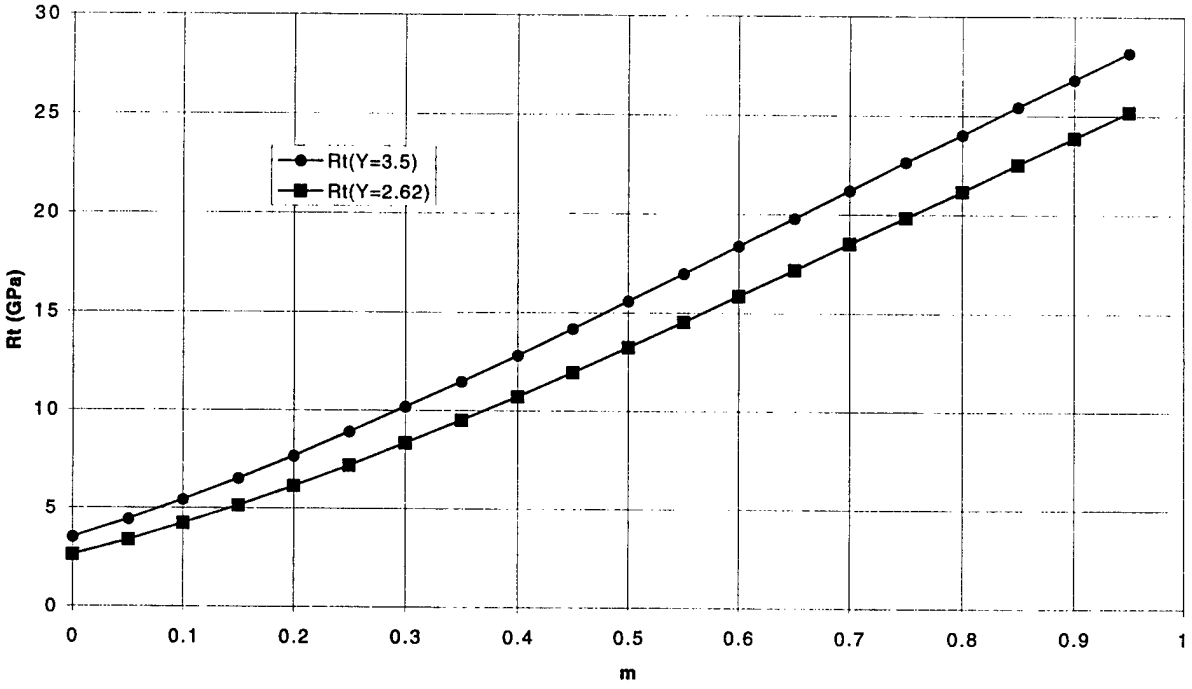

Figure 3. Variation of R_t with pressure-shear coefficient, m.

The radial stress and the shear stress are plotted as a function of normalized radius (r/h) in Figure 4. It can be seen that the pulverized zone and the cracked zone extend to about 3.5 and 9 times the cavity size, respectively. The stresses fall off to zero asymptotically beyond r/h > 15. Thus the assumption of an infinite target is valid if the target to penetrator diameter ratio is at least 15. This is consistent with radial confinement effects as reported by Bless, et al. [20]. We also plot in Figure 5, pressure vs. shear stress in the various regions which depict the path taken by a virgin material as the cavity pressure starts to build up.

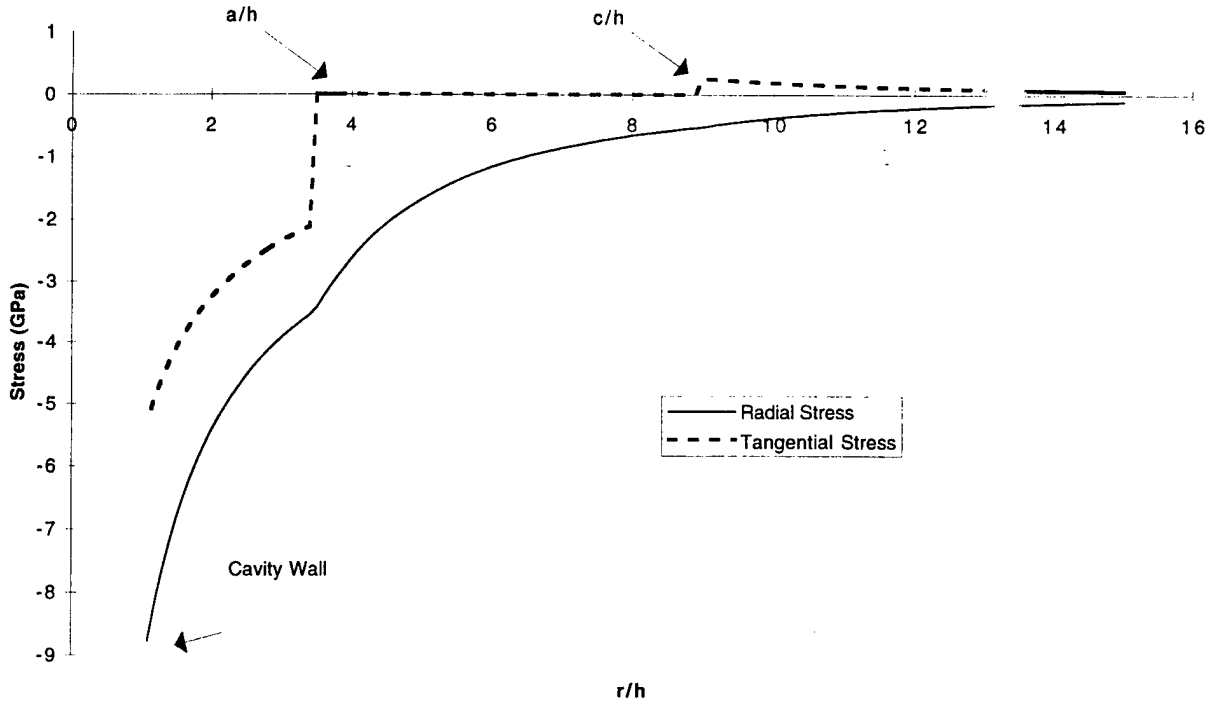

Figure 4. Variation of stresses with normalized radius, r/h.

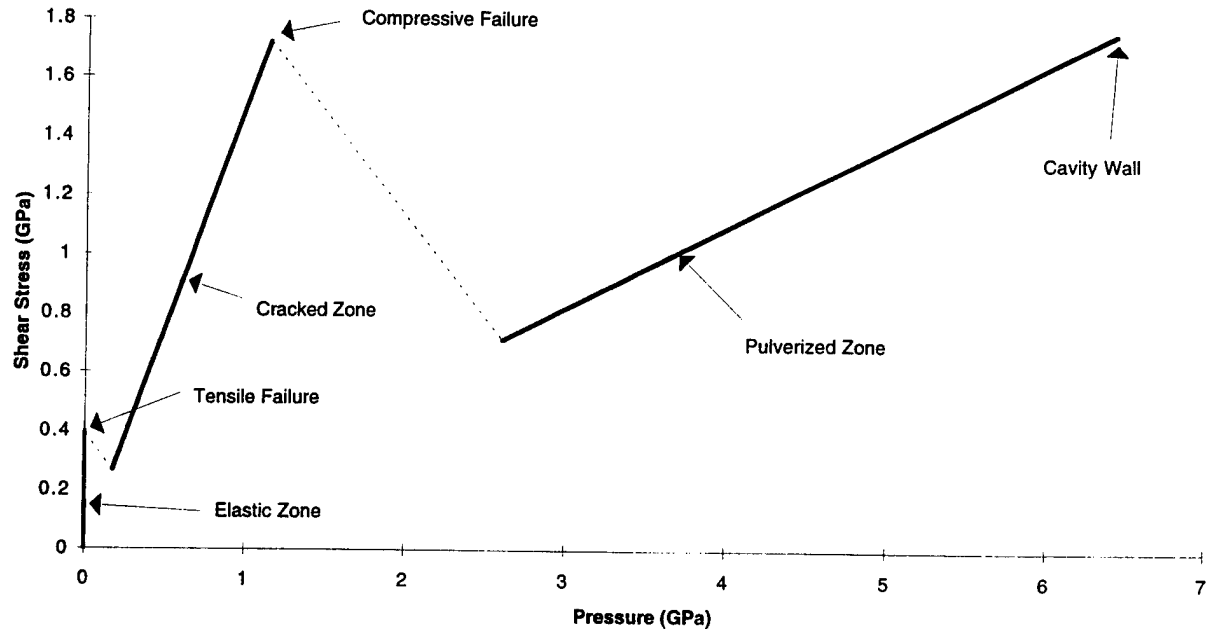

Figure 5. Shear stress vs. pressure in different zones.

10.0 Discussion

This relatively simple treatment has yielded remarkably good correlation with measured R_t values. This is in spite of several weaknesses in the approach, namely: **a)** uncertainty of the measured value of compressive strength; **b)** accuracy of the assumption that material is uniformly comminuted in the pulverized zone; **c)** uncertainty of measured value of pressure-shear coefficient and validity of using this value (which is measured in alumina powder) for a material which has been pulverized from AD995; **d)** inherent assumption of CEM that R_t is due to the pressure required to set up a spherically symmetric stress field ahead of the penetrator; **e)** assumption of no volume change in the pulverized region; and **f)** method of calculating R_t from experimental data by arbitrarily assuming a penetrator strength value and assuming the Tate formulation [19] correctly accounts for inertial stresses.

We feel that the cavity expansion method for study of ceramic penetration has considerable merit and should be pursued further.

Acknowledgments

This work was supported by the U.S. Army Research Laboratory (ARL) under contract DAAA21-93-C-0101.

References

[1] A. Tate, "A Theory for the Deceleration of Long Rods After Impact," *J. Mech. Phys. Solids*, vol. 15, pp. 387-399, 1967.

[2] J. Sternberg, "Material Properties Determining the Resistance of Ceramics to High Velocity Penetration," *J. Appl. Phys.*, vol. 65, pp. 3417-3424, 1989.

[3] R. F. Bishop, R. Hill, and N. F. Mott, "The Theory of Indentation and Hardness Tests," *The Proceedings of Physical Society*, vol. 57, part 3, pp. 147-159, 1945.

[4] M. J. Forrestal, K. Okajima, and V. K. Luk, "Penetration of 6061-T651 Aluminum Targets with Rigid Long Rods," *ASME J. of App. Mech.*, vol. 55, pp. 755-760, 1988.

[5] M. J. Forrestal and D. B. Longscope, "Target Strength of Ceramic Materials for High-Velocity Penetration," *J. Appl. Phys.*, vol. 67, pp. 3669-3672, 1990.

[6] S. C. Wright, Y. Huang, and N. A. Fleck, "Deep Penetration of Polycarbonate by a Cylindrical Punch," *Mech. Mat.*, vol. 13, pp. 277-284, 1992.

[7] Y. Partom, "Ceramic Armor Resistance to Long-Rod Penetration (R_t) and its Dependence on Projectile Velocity," IAT.R 0017, 1993.

[8] R. Subramanium and S. Bless, "Penetration of Semi-Infinite AD995 Alumina Targets by Tungsten Long Rod Penetrators from 1.5 to 3.5 km/s," Hypervelocity Impact Symposium, Santa Fe, NM, October 1994.

[9] Y. Partom and D. L. Littlefield, "Dependence of Ceramic Armor Resistance on Projectile Velocity," Proceedings of the 14th International Ballistics Symposium, Quebec, vol. 2, pp. 563-572, 1993.

[10] F. Collombet and J. Y. Tranchet, "Damage Behavior of Alumina Su itted to a Divergent Spherical Wave," *Journal De Physique IV*, C8-641 - C8-646, 1

[11] D. A. Shockey, A. H. Marchand, S. R. Skaggs, C. E. Cort, M. W. I kett, and R. Parker, "Failure Phenomenology of Confined Ceramic Targets and Imp ng Rods," *Int J. Impact Engng,* vol. 9, pp. 263-275, 1990.

[12] D. R. Curran, L. Seaman, T. Cooper, and D. A. Shockey, "Micromecha al Model for Comminution and Granular Flow of Brittle Material under H Strain Rate Application to Penetration of Ceramic Targets," *Int. J. Impact En* vol. 13, no.1, pp. 53-83, 1993.

[13] R. J. Clifton, M. Ortiz, F. Camacho, and S. Sairam, "Penetration Simulation and Dynamic Response of Comminuted Ceramics," 12th Ceramics Modelling Working Group, held at IAT, Austin, TX, March 1995.

[14] T. Holmquist, private communication, 1995.

[15] D. E. Grady, "Dynamic Properties of Ceramic Materials," Sandia Report, Sand 94-3266.UC-704, 1995.

[16] C. A. Tracy, "A Compression Test for High Strength Ceramics," *Journal of Testing and Evaluation*, vol. 15, no. 1, pp. 14-19, 1987.

[17] N. Brar, S. Bless, and Z. Rosenberg, "Brittle Failure of Ceramic Rods Under Dynamic Compression," *J. de Physique* C-C3, vol. 9, pp. 607-612, 1988.

[18] A. Cosculleula, "Plasticite, Engdommagements, et Ruptures des Alumines Sous Sollicitations Dynamiques Triaxiales: Influence de la Taille des Grains," Thesis, University of Bordeaux I, February 1992.

[19] A. Tate, "Further Results in the Theory of Long Rod Penetration," *J. Mech. Phys. Solids*, vol. 17, p. 141, 1969.

[20] S. J. Bless, R. Subramanian, N. Lynch, and Y. Partom, "Effects of Radial Confinement on the Penetration Resistance of Thick Ceramic Tiles," 15th Int'l Symp Ballistics, Jersusalem, May 21-24, 1995.

Appendix I

Frequently we have to deal with bodies which have cracks, voids, inclusions, etc. All real materials have this kind of inhomogenity, but we intend to neglect these local variations and apply continuum field equations using remote stress-strain conditions. Averaging theorems let us use the continuum equations with volume averaged quantities.

Let us consider a representative volume element (RVE) where external traction t_i^o is prescribed on the boundary which induces the local stress fields, σ_{ij}. Let the stress field as measured on the boundary be $\overline{\sigma}_{ij}$. Now,

$$\int_V \sigma_{ij} dv = \int_V \sigma_{ik}\delta_{kj} dv$$

$$= \int_V \left[\left(\sigma_{ik} x_k\right)_{,k} - \sigma_{ik,k} x_k \right] dv$$

$$= \int_V \left(\sigma_{ik} x_k\right)_{,k} dv \text{ , (since in absence of body force, } \sigma_{ik,k} = 0)$$

$$= \int_S \sigma_{ik} n_k x_j ds, \text{ (using divergence theorem)}$$

$$= \int_S t_i^o x_k ds$$

$$= \int_S \overline{\sigma}_{ij} n_j x_k ds$$

$$= \overline{\sigma}_{ij} \int_v \delta_{jk} dv$$

$$= \overline{\sigma}_{ij} V$$

Hence,

$$\overline{\sigma}_{ij} = \frac{1}{V}\int_V \sigma_{ij} dv$$

Similarly, using a prescribed displacement field on the boundary, it can be shown that the remote strain field, $\overline{\varepsilon}_{ij}$, is related to the local strain field, ε_{ij}, as follows:

$$\overline{\varepsilon}_{ij} = \frac{1}{2V}\int_S \left(u_i n_j + u_j n_i\right) ds = \frac{1}{V}\int_V \varepsilon_{ij} dv$$

Distribution List

Administrator
Defense Technical Information Center
Attn:, DTIC-DDA
8725 John J. Kingman Road, Ste 0944
Ft. Belvoir, VA 22060-6218

Director
US Army Research Lab
ATTN: AMSRL OP SD TA
2800 Powder Mill Road
Adelphi, MD 20783-1145

Director
US Army Research Lab
ATTN: AMSRL OP SD TL
2800 Powder Mill Road
Adelphi, MD 20783-1145

Director
US Army Research Lab
ATTN: AMSRL OP SD TP
2800 Powder Mill Road
Adelphi, MD 20783-1145

Director
Army Research Laboratory
AMSRL-CI-LP
Technical Library 305
APG, MD 21005-5066